

## Supporting Information

# Exploring the influence of the cation type and polymer support in bis(fluorosulfonyl)imide-based plastic crystal composite membranes for CO<sub>2</sub>/N<sub>2</sub> separation

Fernando Ramos,<sup>a</sup> Yady Garcia,<sup>a</sup> Colin Kang,<sup>a</sup> Luke O'Dell,<sup>a</sup> Maria Forsyth,<sup>a</sup> and Jennifer M. Pringle<sup>\*a</sup>

### Thermal analysis

**Table S1.** Thermal data of the neat polymers (PVDF and PEO) and the neat OIPCs ([C<sub>2</sub>mpyr][FSI], [P<sub>1222</sub>][FSI], [HMG][FSI], [N<sub>1111</sub>][FSI], [N<sub>111CN</sub>][FSI]), plus their co-cast composites at different ratios of study (80:20 and 50:50).

	phase III-II		phase II-I		Polymer or combined OIPC/polymer melting		OIPC melting	
	T [°C] ±1°C	ΔH [J g <sup>-1</sup> ] ±10%	T [°C] ±1°C	ΔH [J g <sup>-1</sup> ] ±10%	T [°C] ±1°C	ΔH [J g <sup>-1</sup> ] ±10%	T [°C] ±1°C	ΔH [J g <sup>-1</sup> ] ±10%
PVDF	-	-	-	-	160	33.9	-	-
PEO	-	-	-	-	70	126.6	-	-
[C <sub>2</sub> mpyr][FSI]	-66	33.0	-15	3.7	-	-	203	25.3
80[C <sub>2</sub> mpyr][FSI]-20PVDF	-66	25.1	-16	1.9	140	10.1	198	7.1
50[C <sub>2</sub> mpyr][FSI]-50PVDF	-66	14.3	-15	0.9	143	26.2	-	-
80[C <sub>2</sub> mpyr][FSI]-20PEO	-61	24.0	-14	1.8	62	24.6	203	8.4
50[C <sub>2</sub> mpyr][FSI]-50PEO	-64	6.0	-14	0.6	62	72.6	-	-
[P <sub>1222</sub> ][FSI]	-	-	-52	29.4	-	-	47	23.4
80[P <sub>1222</sub> ][FSI]-20PVDF	-	-	-55	6.6	122	12.0	47	12.0
50[P <sub>1222</sub> ][FSI]-50PVDF	-	-	-53	1.2	142	28.8	48	1.8
80[P <sub>1222</sub> ][FSI]-20PEO	-	-	-51	20.4	53	42.0	-	-
50[P <sub>1222</sub> ][FSI]-50PEO	-	-	-52	1.2	61	67.2	-	-
[HMG][FSI]	10	31.2	67	37.8	-	-	88	6.6
80[HMG][FSI]-20PVDF	10	0.6	68	22.2	115	9.0	85	2.4
50[HMG][FSI]-50PVDF	11	1.2	68	9	132	25.2	86	0.6
80[HMG][FSI]-20PEO	-	-	-	-	62	62.4	-	-
50[HMG][FSI]-50PEO	-	-	-	-	70	101.4	-	-
[N <sub>1111</sub> ][FSI]	-	-	76	51.6	-	-	311	39.0
80[N <sub>1111</sub> ][FSI]-20PVDF	-	-	77	43.2	158	13.8	n/a	n/a
50[N <sub>1111</sub> ][FSI]-50PVDF	-	-	77	21.0	160	36.6	n/a	n/a
80[N <sub>1111</sub> ][FSI]-20PEO	-	-	78	43.2	61	32.4	n/a	n/a
50[N <sub>1111</sub> ][FSI]-50PEO	-	-	77	19.2	64	71.4	n/a	n/a
[N <sub>111CN</sub> ][FSI]	-	-	-66	4.2	-	-	100	74.4
80[N <sub>111CN</sub> ][FSI]-20PVDF	-	-	-65	3.0	165	12.0	103	49.8
50[N <sub>111CN</sub> ][FSI]-50PVDF	-	-	-	-	167	40.8	96	24.6
80[N <sub>111CN</sub> ][FSI]-20PEO	-	-	-65	3.0	53	26.6	101	43.2
50[N <sub>111CN</sub> ][FSI]-50PEO	-	-	-66	1.8	51	66.6	82.4	9.0

### Polarised optical microscopy

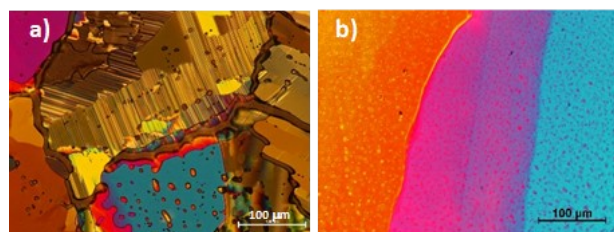


**Figure S1:** Polarized optical micrographs taken at 200x magnification at room temperature after melt and recrystallization on a microscope slide in a hot stage (cooling rate  $10\text{ }^{\circ}\text{C min}^{-1}$ ) of a) neat [HMG][FSI], and b) neat [P<sub>1222</sub>][FSI].

## Gas permeability-selectivity

**Table S2.** CO<sub>2</sub> and N<sub>2</sub> permeability and selectivity of the neat polymers and the OIPC/polymer composites at 35 and 75 °C.

OIPC	Polymer (wt%)	T (K)	P <sub>CO2</sub>	P <sub>N2</sub>	α <sub>CO2/N2</sub>
-	100 PVDF	308	0.7 ± 0.3	0.02 ± 0.003	31 ± 15.8
		348	3 ± 0.1	0.4 ± 0.08	7 ± 0.7
-	100 PEO	308	118 ± 0.5	4.6 ± 1.36	26 ± 8.8
<b>[C<sub>2</sub>mpyr][FSI]</b>	20 PVDF	308	57 ± 5.8	1.3 ± 0.13	43 ± 1.3
		348	95 ± 9.2	5.5 ± 0.50	17 ± 2.7
	50 PVDF	308	63 ± 14.1	4.4 ± 1.95	14 ± 7.0
		348	75 ± 2.2	6.4 ± 0.37	12 ± 1.2
	20 PEO	308	47 ± 1.6	1.4 ± 0.01	33 ± 7.6
	50 PEO	308	54 ± 7.5	2.3 ± 0.01	23 ± 3.3
<b>[P<sub>1222</sub>][FSI]</b>	20 PVDF	308	100 ± 8.3	3.6 ± 0.08	28 ± 2.3
		348	351 ± 51.1	21.8 ± 1.89	16 ± 1.0
	50 PVDF	308	361 ± 5.0	12.4 ± 0.55	29 ± 1.2
		348	479 ± 6.8	36.9 ± 0.51	13 ± 0.0
	80 PEO	308	N/A	N/A	N/A
	50 PEO	308	38 ± 3.2	2.1 ± 0.77	17 ± 6.0
<b>[HMG][FSI]</b>	20 PVDF	308	12 ± 1.7	0.4 ± 0.14	29 ± 5.6
		348	504 ± 59.0	40.6 ± 4.74	12 ± 2.7
	50 PVDF	308	16 ± 7.7	0.6 ± 0.03	26 ± 11.1
		348	279 ± 22.9	21.3 ± 1.07	13 ± 1.8
	20 PEO	308	3 ± 0.4	0.5 ± 0.66	5 ± 7.6
	50 PEO	308	14 ± 0.7	6.8 ± 2.80	2 ± 1.3
<b>[N<sub>1111</sub>][FSI]</b>	20 PVDF	308	1.6 ± 0.0	0.4 ± 0.02	4 ± 0.2
		348	57 ± 0.9	4.9 ± 0.08	11 ± 0.5
	50 PVDF	308	2 ± 1.7	0.9 ± 0.23	3 ± 1.6
		348	29 ± 1.3	4.5 ± 0.21	6 ± 0.5
	20 PEO	308	N/A	N/A	N/A
	50 PEO	308	6 ± 2.4	0.5 ± 0.21	13 ± 2.8
<b>[N<sub>111CN</sub>][FSI]</b>	20 PVDF	308	N/A	N/A	N/A
		348	N/A	N/A	N/A
	50 PVDF	308	5 ± 1.5	0.9 ± 0.11	6 ± 1.8
		348	2 ± 0.2	1.9 ± 0.36	1 ± 1.0
	20 PEO	308	2 ± 0.6	0.7 ± 0.09	2 ± 0.5
	50 PEO	308	N/A	N/A	N/A

## Synchrotron powder X-ray diffraction

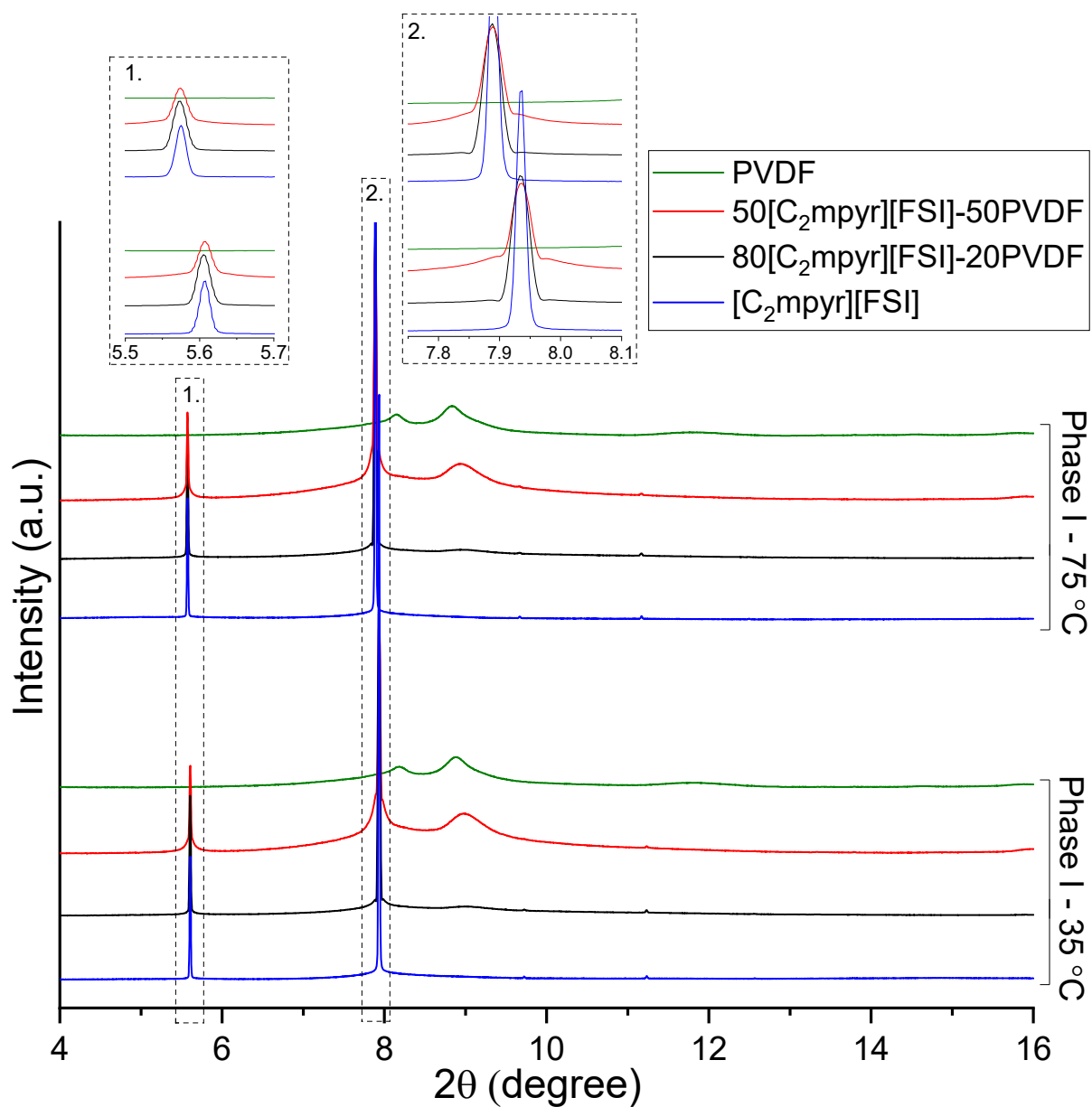


**Figure S2:** Synchrotron powder XRD patterns collected at 35 and 75 °C ( $\lambda = 0.6882361(4) \text{ \AA}$ ) for neat [C<sub>2</sub>mpyr][FSI] (blue), neat PVDF (green) and the composites 80[C<sub>2</sub>mpyr][FSI]:20PVDF (black), and 50[C<sub>2</sub>mpyr][FSI]:50PVDF (red). Details of the peaks are magnified and numbered.

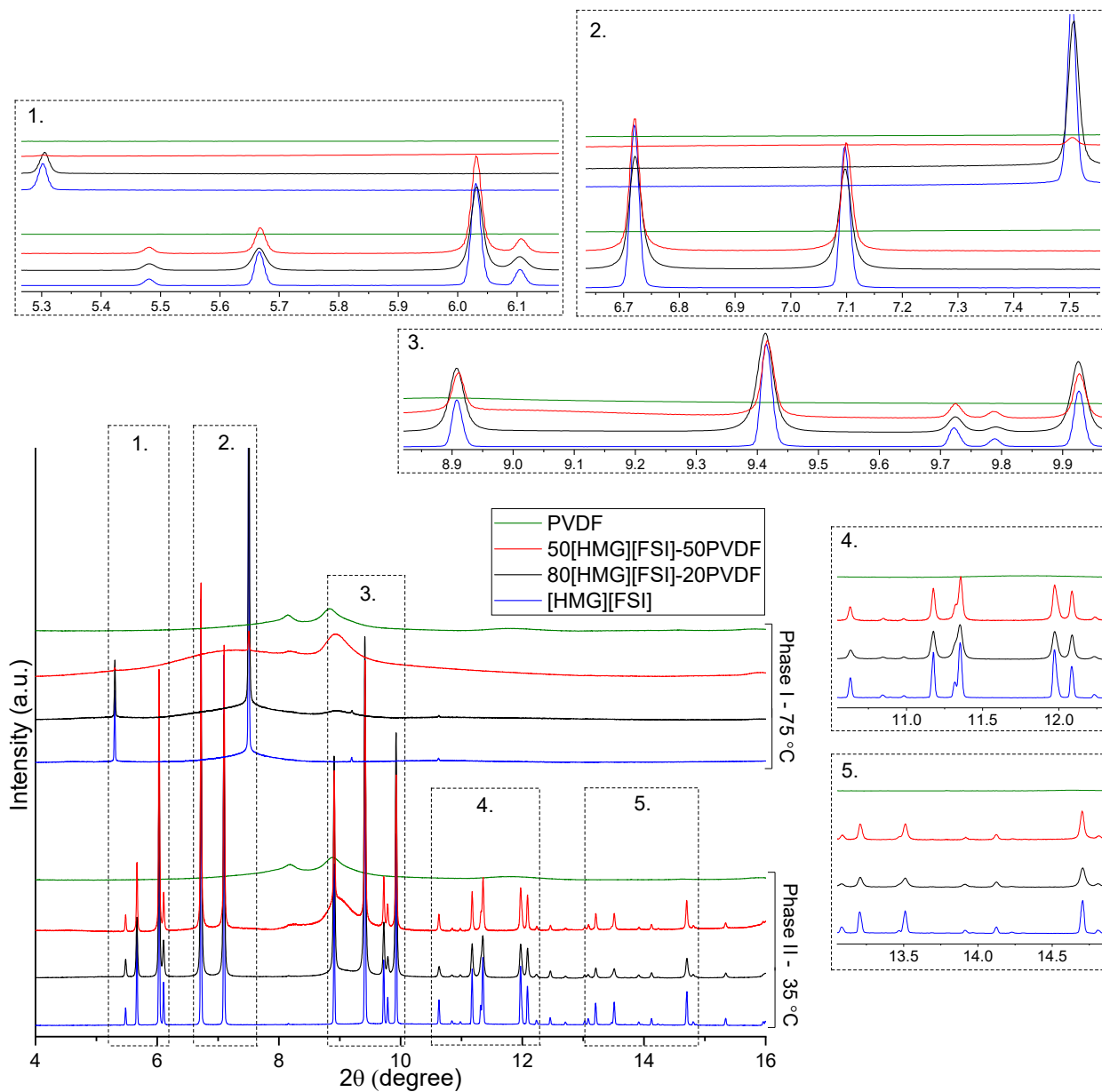


**Figure S3:** Synchrotron powder XRD patterns collected at 35 and 75 °C ( $\lambda = 0.6882361(4)$  Å) for neat [HMG][FSI] (blue), neat PVDF (green) and the composites 80[HMG][FSI]:20PVDF (black), and 50[HMG][FSI]:50PVDF (red). Details of the peaks are magnified and numbered.

## Line width (FWHMs) and Area fraction of narrow peak

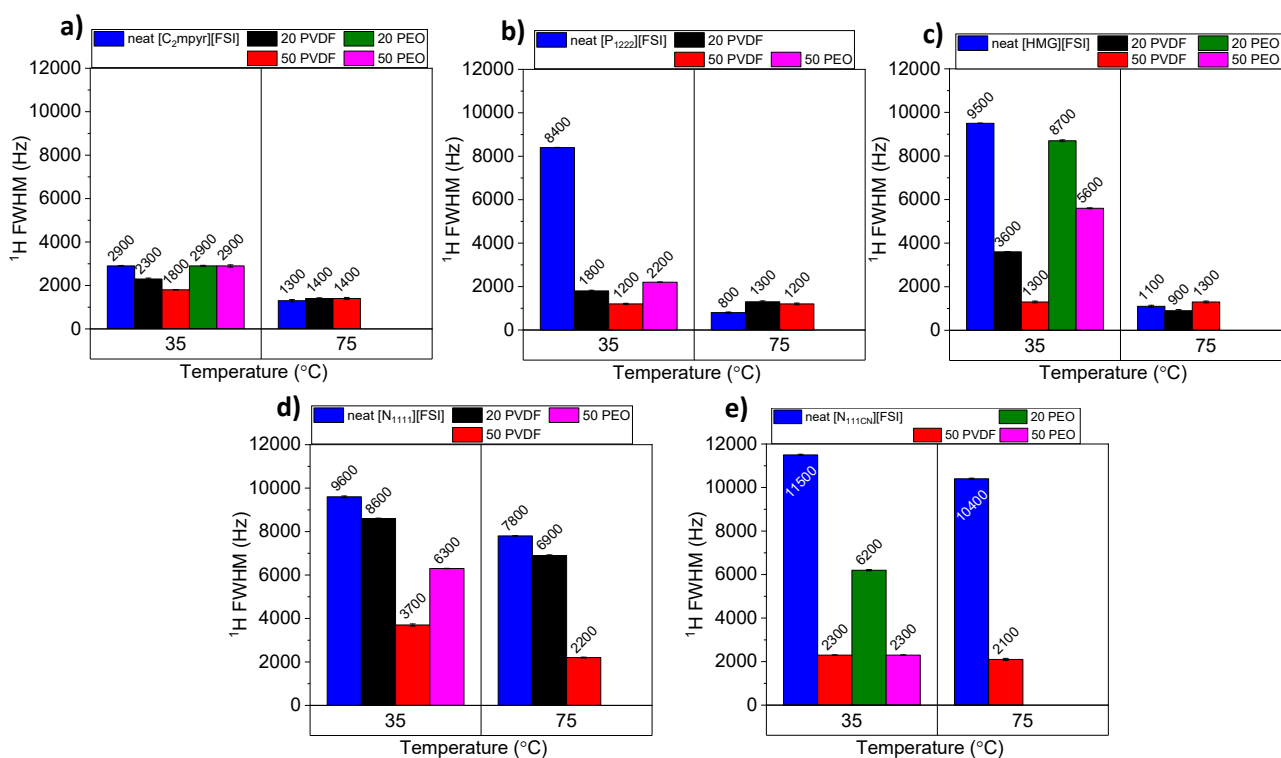


**Figure S4.**  $^1\text{H}$  Line full width at half-maximum (FWHMs) b) neat [P<sub>1222</sub>][FSI], c) neat [HMG][FSI], d) neat [N<sub>1111</sub>][FSI], e) neat [N<sub>111CN</sub>][FSI], and their corresponding PVDF and PEO composites.

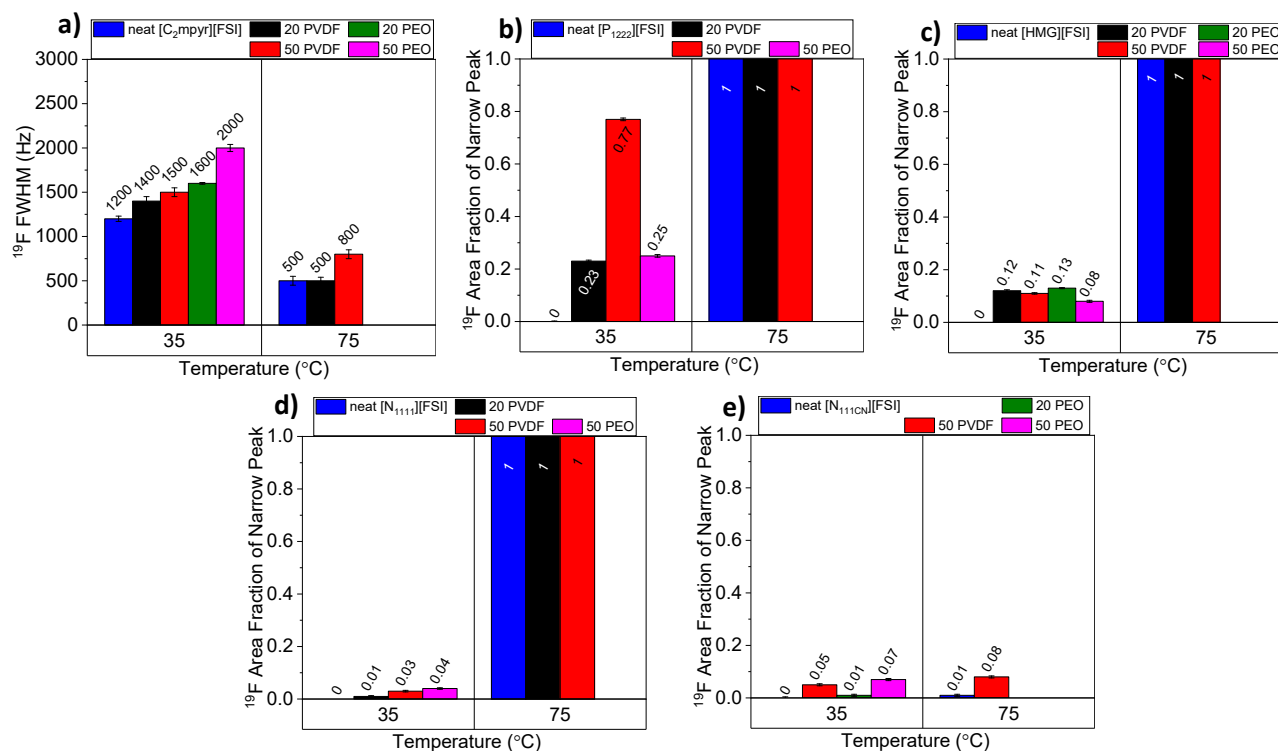
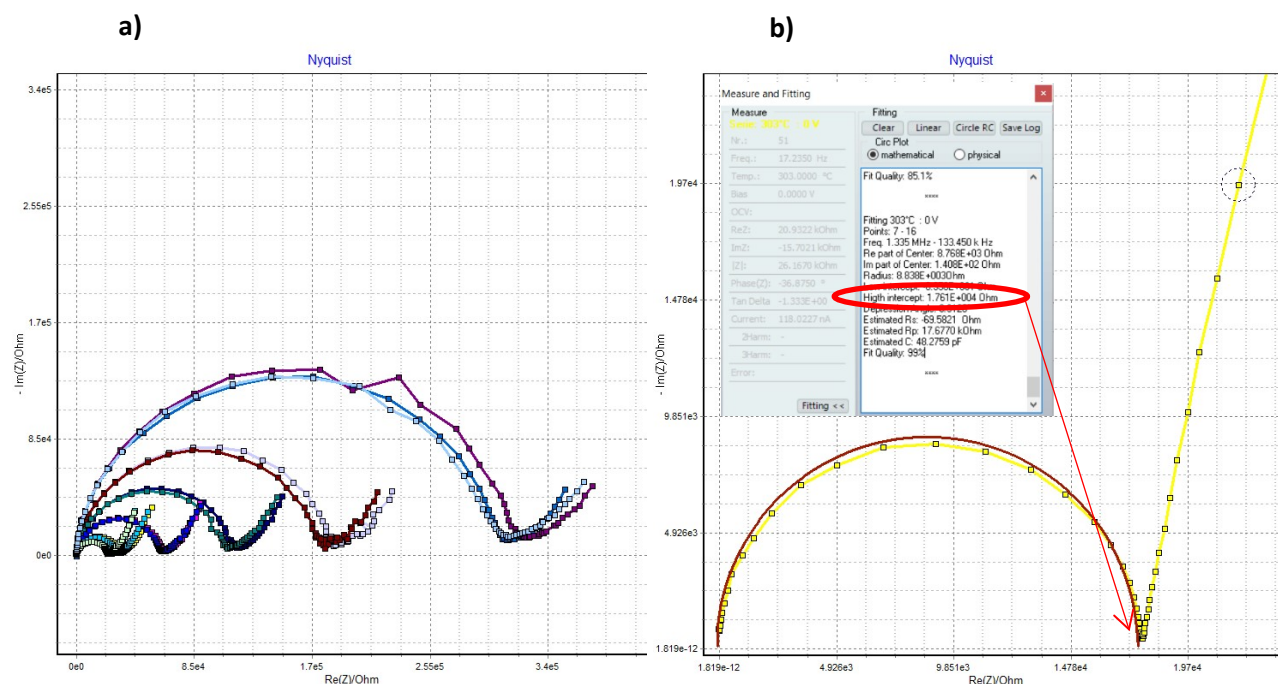


**Figure S5.** a)  $^{19}\text{F}$  Line full width at half-maximum (FWHMs) of neat [C<sub>2</sub>mpyr][FSI] and its PVDF and PEO composites.  $^{19}\text{F}$  Area Fraction of Narrow Peak of: b) neat [P<sub>1222</sub>][FSI], c) neat [HMG][FSI], d) neat [N<sub>1111</sub>][FSI], e) neat [N<sub>111CN</sub>][FSI], and their corresponding PVDF and PEO composites.

**Table S3.** Fitting parameters of the fluorine nuclei in the OIPCs. The parameters of the FSI anion were extracted from  $^{19}\text{F}$  NMR spectra of the pure OIPCs at  $35^\circ\text{C}$  by iterative fitting to a simulated CSA pattern and gauss/Lorentzian line shape function using the DMfit software.

OIPC	Model	Chemical shift (ppm)	Relative Intensity	$\delta(\text{CSA})$	$\eta(\text{CSA})$
[C <sub>2</sub> mpyr][FSI]	gauss/Lorentzian	95.6	1	-	-
[HMG][FSI]	CSA	95.8	1	-73.51	0.99
[P <sub>1222</sub> ][FSI]	gauss/Lorentzian	95.6	0.01	-	-
	CSA	94.2	0.99	49.5	0.14
[N <sub>1111</sub> ][FSI]	CSA	91.5	1	-129	0.46
[N <sub>111CN</sub> ][FSI]	gauss/Lorentzian	93.9	0.00	-	-
	CSA	94.3	0.1	78.85	0.26

Surprisingly, the [FSI]<sup>-</sup> anions exhibit very different CSA pattern shapes depending on the OIPC cation. The CSA line shapes are quantified by parameters including the asymmetry parameter ( $\eta$ ) which indicates how much the environment around the fluorine nucleus deviates from axial symmetry and takes values between 0 and 1.<sup>1</sup> The shape of the [P<sub>1222</sub>][FSI] CSA pattern presents a CSA asymmetry parameter ( $\eta$ ) near zero ( $\sim 0.14$ ) and suggests that fluorine atoms have an axially symmetry in the [FSI] anion. The value of  $\eta$  increases, [N<sub>111CN</sub>][FSI] < [N<sub>1111</sub>][FSI] < [HMG][FSI], and indicates a deviation of the axially symmetry of the fluorine in these OIPCs (Figure 9)(Table S3). These differences are a result of the symmetry, size and packing of cations that surround them.



### Electrochemical impedance spectroscopy (EIS)

**Figure S6.** a) Example of Nyquist plot acquisition over a temperature range in neat [HMG][FSI] pellet. b) Example of Nyquist plot fitting to obtain resistance value of 50[C<sub>2</sub>mpyr][FSI]:50PVDF.

## References SI

- [1] H. W. Spiess, in *Dynamic NMR Spectroscopy* (Eds.: A. Steigel, H. W. Spiess), Springer Berlin Heidelberg, Berlin, Heidelberg, **1978**, pp. 55-214.